Environment Protection Engineering

Vol. 49 2023 No. 3

DOI: 10.37190/epe230305

RURU LIANG[1], GUANGLEI YUAN[1], RENPING LIU[1], ERHONG DUAN[1, 2], JIALE SONG[1]

EFFECTS OF CO-DISPOSAL OF SLUDGE BASED ON TTF-TYPE PRECALCINER ON NO_x EMISSIONS

To reduce the emission of nitrogen oxides (NO_x) during the co-disposal of sludge in a TTF-type precalciner, an optimized co-disposal process of a TTF-type precalciner has been implemented in a cement plant in Hebei. The model was built using ANSYS FLUENT software. The effects of three single-factor perspectives (sludge input ratio, gas flow rate, and tertiary air temperature on NO concentration) were investigated. The response surface method of Box–Behnken design was used. When the sludge ratio increased from 0 to 25%, the NO concentration at the outlet was 122–297 mg/m³. Meanwhile, it increased from 192 mg/m³ to 241 mg/m³ since the airflow increased from 95 m³/s to 122 m³/s. The maximum NO concentration was 192 mg/m³ when the tertiary air temperature was 1170 K. The interaction between airflow and sludge ratio was more significant than any other interaction between other conditions ($P < 0.05$). Finally, the optimum conditions were a sludge ratio of 5%, airflow 109 m³/s, and tertiary air temperature 1280 K. NO concentration was 166.9 mg/m³ under this condition.

1. INTRODUCTION

In recent years, China's waste-water treatment capacity has grown by leaps and bounds, leading to increased production of municipal sludge [1]. Municipal sludge contains many parasitic eggs, pathogenic microorganisms, and toxic heavy metals which can cause great environmental hazards if not treated in time [2].

Common sludge disposal technologies such as landfills, composting, and ocean dumping, are limited due to environmental protection policies and high costs [3]. Co--disposal technology in the cement industry is an eco-friendly disposal method, which is widely used in the United States and Europe. Since 2016, our government has started to encourage cross-industry co-disposal of solid waste. Production lines have been built

[1]College of Environmental Science and Engineering, Hebei University of Science and Technology, Shijiazhuang 050018, China, corresponding author R. Liu, email address: pingrenliu@163.com

[2]National Joint Local Engineering Research Center for Volatile Organic Compounds and Odorous Pollution Control, Shijiazhuang 050018, China.

for the co-disposal of sludge in cement plants one after another, due to its advantages of thorough disposal, heavy metal melting [4] and solidification, low investment, etc. However, it is worth noting that sludge contains N compounds, organic matter, and other substances. As a result, the impact of the co-disposal of municipal sludge on NO_x emissions in the cement industry is complex [5].

Fuel NO_x, which is produced from nitrogen in the fuel, makes up the majority of the NO_x at temperatures between 850 and 1000 °C. Volatile nitrogen is transformed during fuel combustion into the intermediate products HCN and NH_3, which are then oxidized to NO. Coke is oxidized to NO while the unoxidized intermediate molecules continue to interact with NO to create N_2 [6]. However, coke is reductive and part of NO is reduced to N_2 [7]. The specific transformation relationship is as follows in Fig. 1. Since NO accounts for more than 90% of fuel-based NO_x, the amount of fuel NO is generally considered as the amount of NO_x emissions.

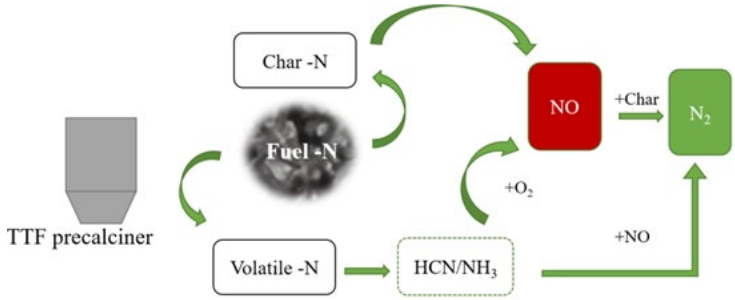

Fig. 1. N relation transformation

Compared with coal, sludge has a higher volatile fraction. However, its fixed carbon and calorific value are lower, which makes it more possible to emit NO_x during co--disposal. Shimizu et al. [8] suggested that ash in sludge combustion promoted NO_x production, Some authors [9] suggested that sludge feeding amount, sludge particle size, cement raw material and its composition, and additive species played an important role in NO_x removal. Lv et al. [10] suggested that NH_3 released from sludge increased the NH_3 content in the decomposer and had a facilitating effect on the reduction of NO. It is noteworthy that other studies on NO_x emissions showed that it can still be reduced by adjusting the decomposer operating parameters. Fang et al. [11] found that combustion temperature, gas flow rate, and oxygen concentration also had significant effects on NO_x removal. Xiao et al. [12] conducted an experimental study on the effect of CO_2 concentration on NO reduction efficiency by sludge reignition in a cement decomposer. When the CO_2 concentration was 25 vol. %, the optimum NO reduction rate reached 54%.

In the process of co-disposal of sludge, the main source of NO_x emission is the combustion of fossil fuels in the furnace and the chemical reaction of raw materials under high-temperature conditions [13]. The process parameters of the decomposer on

NO emission can be studied by optimizing the combustion system of the decomposer and by adjusting the airflow, tertiary airspeed, and other conditions. The change of tertiary air temperature changes the temperature distribution in the furnace and affects NO_x emission. Therefore, it is important to study the influence of cement decomposers on NO_x emission after sludge addition. Therefore, it is important to study the influence of NO_x emission on cement decomposers after sludge addition. However, so far, there are limited studies on adjusting the operation process to optimize NO_x emission of cement decomposers based on the co-disposal of sludge, and there are even fewer studies on the influence of various factors on NO_x emission.

In this study, a cement decomposition furnace of TTF type in a cement plant in Hebei Province is selected as the research object to establish the model. Additionally, ANSYS FLUENT software was used to determine the sludge input ratio of 0, 5, 10, 15, 20, and 25%, the airflow of 95, 102, 109, 115, and 122 m^3/s, and the tertiary temperatures of 1170, 1200 1220, 1250, and 1280 K. Besides, other conditions were studied by numerical simulation. Based on the single-influence study, the response surface analysis method (RSM) was further employed to improve the NO_x emission system in the co-disposal of sludge from a multi-factor perspective. The study's findings offer a theoretical framework and a model for predicting NO levels that may be used to optimize the NO_x emission system during the co-disposal of sludge in cement plants.

2. NUMERICAL METHOD

2.1. MATHEMATICAL MODEL

The *K*-ε model is most frequently employed in general turbulence numerical simulation to represent the turbulence of gas flow. The standard *K*-ε model is easier to converge [14], and the specific formula is as follows:

$$\frac{\partial(\rho k)}{\partial t}+\frac{\partial(\rho uk)}{\partial x}+\frac{\partial(\rho vk)}{\partial y}+\frac{\partial(\rho wk)}{\partial z}=\frac{\partial}{\partial x}\left(\left(\mu+\frac{\mu_t}{\sigma_k}\right)\frac{\partial k}{\partial x}\right)$$

$$=\frac{\partial}{\partial y}\left(\left(\mu+\frac{\mu_t}{\sigma_k}\right)\frac{\partial k}{\partial y}\right)+\frac{\partial}{\partial z}\left(\left(\mu+\frac{\mu_t}{\sigma_k}\right)\frac{\partial k}{\partial z}\right)+\rho G_k-\rho\varepsilon$$

where ρ is density, k is turbulent kinetic energy, ε is turbulent dissipation, G_k is velocity gradient generation term, μ_t is eddy viscosity, $\mu_t=\rho C_\mu(k^2/k\varepsilon)$, $C_\mu=0.09$ is a constant.

When pulverized coal and municipal sludge particles interact with the gas in the furnace, they are rapidly heated and undergo transformation processes [15]. To simulate the volatilization processes in coal and municipal sludge, a two-competing-rates model

is used [16]. The model uses two first-order equations to control the reactions at low and high temperatures, respectively:

$$\text{coal/sludge} \xrightarrow{k_1} \alpha_1 \text{ Volatile}_1 \text{ (g)} + \beta_1 \text{ Char}_1 \text{ (s)}$$

$$\text{coal/sludge} \xrightarrow{k_2} \alpha_2 \text{ Volatile}_2 \text{ (g)} + \beta_2 \text{ Char}_2 \text{ (s)}$$

$$k_1 = A_1 \exp\frac{E_1}{RT_p}, \quad k_2 = A_2 \exp\frac{E_2}{RT_p}$$

where k_1 and k_2 are the competitive volatilization rates at low and high temperatures, E_1 and E_2 activation energies [16], A_1 and A_2 pre-exponential factors, and T_p particle temperature.

The complex combustion process of coke in a decomposer is influenced by various factors such as fuel structure, decomposer temperature, and pressure. Raised by Baum and Street [17] and Field [18], the kinetic/diffusion-limited model was used in the process. The reaction rate is determined by the diffusion rate of the gaseous oxidant to the particle surface and the internal reaction kinetics [19]. The following equation gives the burning rate of coke

$$R_1 = C_1 \frac{\left(\frac{T_p + T_\infty}{2}\right)^{0.75}}{d_{p,}}, \quad R_2 = C_2 \exp\left(-\frac{E}{RT_p}\right)$$

where R_1 is diffusion rate, R_2 kinetic rate, T_∞ ambient gas temperature, C_2 pre-exponential factor, 0.0059 kg/(m^2·s·Pa), d_p particle diameter and E activation energy.

The coupling between the fuel particles and the gas phase is modeled using a discrete phase model, which is built using Lagrangian coordinates [20]. The control equations for the Cartesian coordinates are as follows

$$\frac{du_p}{dt} = F_D\left(u - u_p\right) + \frac{g_x\left(\rho_p - \rho\right)}{\rho_p} + F_x$$

where u is fluid phase velocity, u_p particle phase velocity, ρ_p particle density F_x other acting force, $F_D(u - u_p)$ the traction force per unit mass of the particle, where

$$F_D = \frac{18\mu}{\rho_p d_p^2} \times \frac{C_D Re}{24}$$

and Re is the relative Reynolds number defined as

$$Re = \frac{\rho d_p \left| u_p - u \right|}{\mu}$$

The traction coefficient C_D is

$$C_D = \alpha_1 + \frac{\alpha_2}{Re} + \frac{\alpha_3}{Re}$$

where for spherical particles, α_1, α_2 and α_3 are constants in the field of certain Reynolds numbers ($\alpha_1 = 0.28$, $\alpha_2 = 6$, $\alpha_3 = 21$).

Species transport models can be used to solve for species transport processes and chemical reactions [21], including wall chemical reactions and combustion.

The conservation equation takes the following general form

$$\frac{\partial}{\partial t}\left(\rho Y_i\right) + \nabla\left(\rho \vec{v} Y_i\right) = -\nabla \vec{J}_l + R_i + S_i$$

In this study, Finite-Rate/Eddy-Dissipation is chosen for the chemical reactions involved in the furnace. Therefore, the Arrhenius equation and the vortex dissipation equation are calculated simultaneously, combining the kinetic and turbulence factors with the following equation

$$W = KC_A^a C_B^b = K_0 \exp\left(-\frac{E}{RT}\right) C_A^a C_B^b$$

$$R_{i,r} = V'_{i,r} M_{w,i} AB\rho \frac{\varepsilon}{K} \times \frac{\sum_P Y_P}{K \sum_j^N V''_{j,r} M_{w,j}}$$

where C_A and C_B are reactant concentrations, a, b are stoichiometric numbers, K_0 is pre-exponential factor, $V'_{i,r}$ is the stoichiometric number of reactant i in reaction r, Y_P product mass fraction, A and B are reaction constants (generally $A = 4$, $B = 0.5$), $V''_{j,r}$ the stoichiometric number of product j in reaction r, and $M_{w,i}$ molecular weight of product i.

In the precalciner, radiative heat transfer accounts for more than 95% of the heat transfer in the furnace chamber. For the calculation, the P1 radiation model is chosen. The radiation heat transfer equation is as follows

$$\frac{Q_e}{Q}+\frac{Q_r}{Q}+\frac{Q_d}{Q}=1$$

$$q_r=\frac{dQ}{dt}=-\frac{1}{\alpha+\sigma_s-c\sigma_s}\nabla G$$

The transport equation for G is

$$\nabla\left(I\nabla G\right)-aG+4an^2\sigma T^4=S_G$$

$$-\nabla q_r=aG-4an^2\sigma T^4$$

where Q_e/Q is absorbance, Q_r/Q reflectance, Q_d/Q transmittance, q_r radiation flux, and α absorption, σ_s is scattering coefficient, G incident radiation, C linear anisotropic phase function coefficient, n refractive index of the medium, σ Boltzmann constant, and S_G user-defined radiation source.

Since the generation of NO in the precalciner is small, and the influence on the component fields such as flow rate and temperature is also small, the post-treatment method is chosen for the calculation [6].

2.2. GEOMETRIC MODEL

This paper is based on a new dry process cement production line TTF type precalciner in the northwest of Shijiazhuang City, Hebei Province, which has a production capacity of 5000 t per day. The dimensions and structure of the precalciner are shown in Fig. 2.

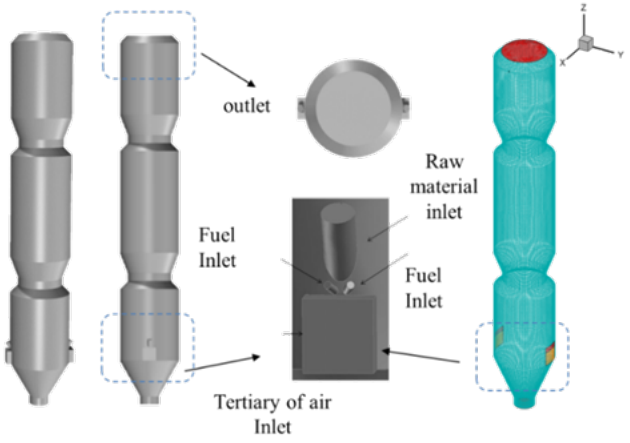

Fig. 2. Precalciner structure

TTF-type precalciner has three sections and two indents, consisting of the first mixing chamber, the second mixing chamber, and the combustion chamber. The diameter of the column is 7.1 m, the diameter of the top and bottom two indentations is 5.1 m, the diameter of the bottom cone-shaped flue gas inlet is 2.4 m, and the diameter of the top outlet is 5.3 m. There are two inlets of the third air, located at 6.5 m from the flue gas inlet, with an inlet area of 3.4 m^2 and symmetrically distributed, and the inlet of pulverized coal and raw material are located in the upper part of the third air, symmetrically distributed on both sides of the first column, and the inlet of pulverized coal is slanted downward with the horizontal direction at an angle of 25° angle. When the three winds blow in and the bottom flue gas meet, they will produce a vortex with the first spraying effect. After that two contractions in the pre-calciner indentation produce the second and third spraying effect, increasing the degree of particle mixing, extending the residence time of particles, and making the reaction more complete.

2.3. BOUNDARY CONDITIONS AND MESH-INDEPENDENT TESTS

The particle phase injection was used to inject the fuel into the interior of the precalciner. The boundary exit condition was set to escape and three air inlets and the flue gas inlet are set to velocity inlet. Meanwhile, the outlet is set to pressure outlet, and the boundary conditions are defined as wall except for the fuel inlet, fuel gas, three air inlet, and total outlet.

According to the basic working data of the cement plant, the analysis of municipal sludge, coal industry, and basic boundary condition data of the numerical simulation are listed in Tables 1 and 2.

Table 1

Results of industry and elemental analyses of municipal sludge and coal [%]

Item	Industry analysis				Elemental analysis			
	M	V	Fc	A	C	H	O	N
Sludge	9.21	59.44	2.79	28.56	43.82	7.54	40.52	8.12
Coal	10	25	50	15	75	5	4	1

M, A, V, and Fc are moisture, volatile matter, ash, and fixed carbon, respectively.

Table 2

Boundary parameters

Boundary	Mass flow rate [kg/s]	Velocity [m/s]	Temperature [K]
Flue gas inlet	50.46	–	1399
Raw material inlet	59.93	–	1035
Tertiary air inlet	–	30	1173

The simulation results of 279 930, 367 602, 414 770, and 641 556 grid numbers under similar conditions (Table 3) show that the simulation gap between the grid numbers is small, and the next experiments take 279930 grids for the study.

Table 3

Mesh-independent verification without sludge input

Mesh number	Parameters		
	Temperature [K]	O_2 mole fraction [%]	Velocity [m/s]
279 930	1255.441	0.59	24.98906
367 602	1248.982	0.68	25.15590
414 770	1249.982	0.57	25.24372
641 556	1244.797	0.60	25.10652

2.4. VERIFICATION OF THE MODEL

Simulated and calculated values of the temperature, NO concentration, and raw material decomposition rate are given in Table 4. It can be seen that the error is not large, and the model established is correct.

Table 4

Model correctness verification

Values	Temperature [K]	Raw material decomposition rate [%]	NO concentration [mg/m^3]
Actual	1196	85–89	496
Simulated	1249	84.99	526

3. IMPACT FACTOR

The sludge addition ratio, airflow, and tertiary air temperature have been selected from the factors affecting NO emission in the precalciner. The sludge input ratio changed the fuel composition in the furnace, which further affected the NO emission. The airflow and tertiary air temperature affected the combustion. Figure 3b shows that the NO concentration at the exit is significantly influenced by the sludge input ratio and ranges from 122 to 297 mg/m^3. From Fig. 3a, it can be seen that as this sludge input ratio increases, the NO concentration also shows an increasing trend, which is due to the high N content [22] and a volatile fraction of the sludge and NO concentration. But when the sludge input ratio reaches 25%, the NO_x concentration slightly decreases. That is because NO_x precursor substances such as HCN and NH_3 are produced when sludge is added in excess, which may cause some NO_x to undergo reduction reactions [23]. In the co-disposal of municipal sludge by precalciner on NO_x emission, 5% and 15% are the better optimization results.

$$4NH_3 + 5O_2 \rightarrow 4NO + 6H_2O$$

$$4HCN + 7O_2 \rightarrow 4CO_2 + 2H_2O$$

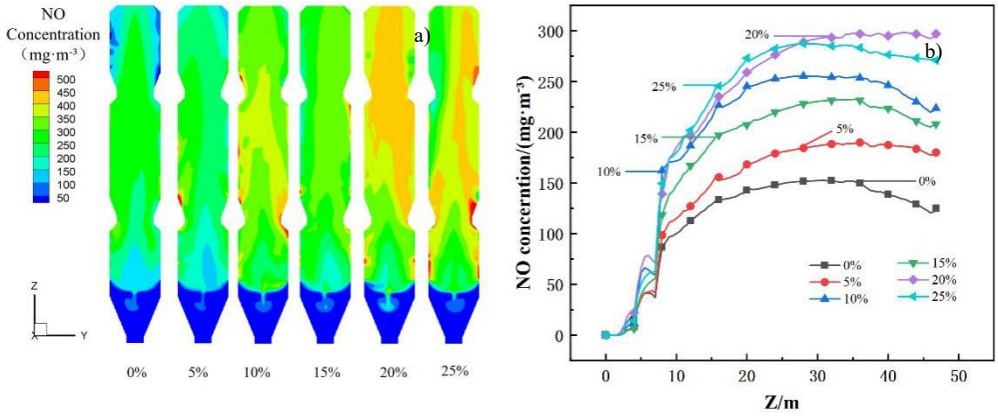

Fig. 3. Effects of sludge input ratio on temperature (a) and NO concentration along the *z*-axis

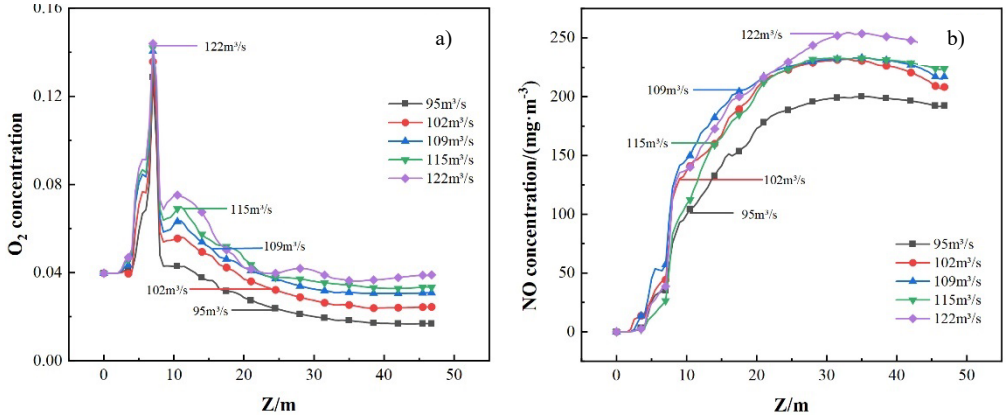

Fig. 4. Effects of airflow on O_2 (a) and NO (b) concentrations along the *z*-axis

The effects of different airflows on the NO concentration in the direction of the precalciner *z*-axis are shown in Fig. 4b. It can be seen from Fig. 4a that as the airflow rate increases, the oxygen content increases, and the molar fraction of oxygen at the outlet is 0.017–0.039. The NO concentration at the exit of the precalciner is 192–241 mg/m³. A small air coefficient denotes inadequate oxygen and ventilation, which leads to incomplete combustion. The NO concentrations of the fuel and the oxygen level in the combustion zone both affect how much NO is produced. Further, sufficient oxygen allows full combustion of the fuel [24]. Volatile fraction of NO conversion increases with the increasing oxygen concentration.

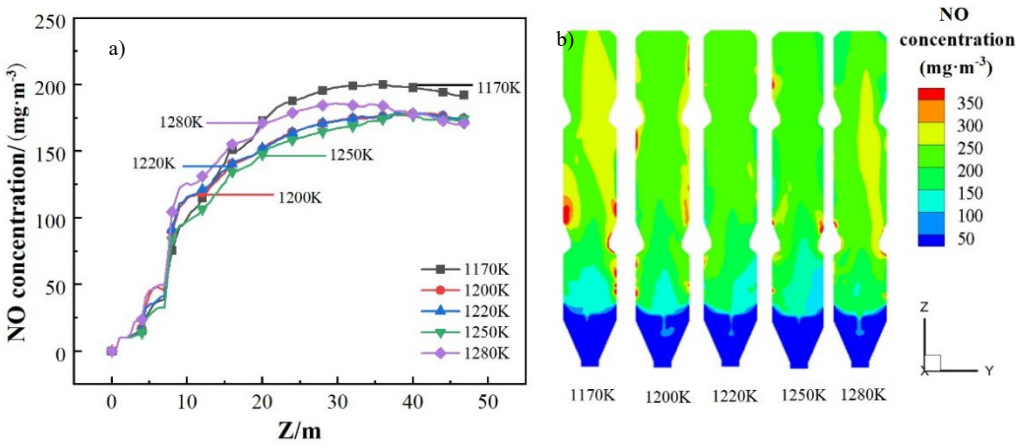

Fig. 5. Effect of tertiary air temperature on NO concentration along the *z*-axis (a) and concentration distributions of NO at different tertiary air temperatures (b)

The impacts of various tertiary air temperatures on the concentration of NO in the precalciner *z*-axis are shown in Fig. 5a. The concentration of NO at the exit decreases upon increasing temperature. At 1170 K, the concentration of NO at the outlet has a maximum value of 192.31 mg/m³. However, the differences in NO concentrations under other conditions are not significant, due to the increase of temperature. By prompting the fuel to burn fully, releasing more HCN and NH_3, and reducing NO to some extent a contributing decrease in NO concentration occurs. It is also clear from Fig. 5b that a trend of decreasing NO concentration compared to that at the tertiary air temperature of 1170 K.

4. DESIGN OF RESPONSIVE SURFACES

The studies mentioned above are all trials on individual influencing factors, making it difficult to achieve the desired optimization result. As a result, in this section, a three--factor and three-level response surface analysis experiment has been conducted. The sludge ratio, airflow, and tertiary air temperature have been employed as three independent variables, and NO_x content as the response value, based on the single factor experiments described above. Table 5 displays the experiment parameters and levels.

Table 5

Experimental factors

Factor		Level		
		–1	0	1
Ratio, %	X_1	5	10	15
Airflow, m³/s	X_2	95	109	122
Tertiary air temperature, K	X_3	1170	1225	1280

4.1. RESPONSE EQUATION ESTABLISHMENT AND ANALYSIS

The experimental factors and levels (Table 6) were designed using Design Expert software. The experimental serial numbers were randomly generated.

Table 6

Experimental design

Number	X_1 [%]	X_2 [m³/s]	X_3 [K]	Y [mg/m³]
1	–1	–1	0	166.7
2	0	–1	1	180.6
3	0	–1	–1	170.6
4	1	–1	0	211.2
5	0	1	–1	232.2
6	–1	0	1	166.9
7	–1	0	–1	199.9
8	0	0	0	185.8
9	0	0	0	186.0
10	0	0	0	186.0
11	0	0	0	185.5
12	0	0	0	185.6
13	–1	1	0	207.3
14	1	0	–1	229.4
15	1	0	1	235.4
16	1	1	0	294.4
17	0	1	1	211.3

Multiple regression analysis and binomial fitting were performed on the factors and response values to obtain the model equation of NO concentration response surface:

$$y = 185.11 + 28.79X_1 + 27.48X_2 - 4.59X_3 + 9.54X_1X_2 + 9.47X_1X_3 - 7.78X_2X_3 + 21.46X_1^2 + 12.33X_2^2 + 0.76X_3^2$$

The second-order model ANOVA is presented in Table 7. The significance test of the model is $P < 0.0001$, and the misfit term is $P < 0.0001$. Both the regression model and the misfit are statistically significant. The corrected coefficient of determination R^2 of the model is 97.78% [25], which indicates that this model can explain 97.78% of the variation of the response value, and the fit with the actual experiment is relatively good. Adeq precision is much greater than 4, which proves that the model has a high degree of credibility. The resulting analysis and scheme optimization can be carried out based on the model to clarify the optimal process for NO emission reduction.

Table 7

Results of analysis of variance of a second-order model

Source	Sum of squares	*Df*	Mean square	*F* value	*P* value
Model	15 864.8	9	1762.76	34.19	<0.0001
Lack of fit	360.69	3	120.23	2226.86	<0.0001
Pure error	0.22	4	0.054		
Cor total	16 225.71	16			

$R^2 = 0.9778 R^2(\text{adj}) = 94.92\%$.
$P < 0.05$ has a significant effect and $P < 0.01$ has a highly significant effect.

From the factor significance experiments (Table 8) it can be seen that X_1 (ratio) plays a highly significant effect on NO emission, similarly to X_2 (airflow). The interaction terms X_1X_2 and X_1X_3 (tertiary air temperature) both have relatively significant effects on NO emission.

Table 8

Factor significance test

Term	Coefficient	*Df*	Standard error	95% *CI* low	95% *CI* high	*P*
Intercept	185.77	1	3.21	178.18	193.36	
X_1	28.70	1	2.54	22.70	34.70	<0.0001
X_2	25.77	1	2.54	19.77	31.77	<0.0001
X_3	–5.99	1	2.54	–11.99	0.017	0.0505
X_1X_2	10.66	1	3.59	2.17	19.15	0.0208
X_1X_3	9.74	1	3.59	1.25	18.23	0.0301
X_2X_3	–5.21	1	3.59	–13.70	3.28	0.1901
X_1X_1	20.43	1	3.50	12.15	28.70	0.0006
X_2X_2	13.70	1	3.50	5.43	21.97	0.0058
X_3X_3	1.70	1	3.50	–6.57	9.98	0.6411

4.2. RESPONSE SURFACE ANALYSIS

The relationships among sludge ratio, airflow, tertiary air temperature, and NO concentration at the outlet of the precalciner are shown in Figs. 6–8. The contour and response surface plots of the sludge input ratio interaction are shown in Fig. 6. It is clear from Fig. 6a that the interaction term significantly affects the response values. As demonstrated in Fig. 6b, the NO concentration tends to increase as the airflow rate increases at a constant sludge input ratio. However, when the airflow is steady, the NO concentration increases as the sludge input ratio increases which confirms our previous findings.

The dependences of the tertiary air temperatures and airflow on the NO concentration are shown in Fig. 7. When the airflow is constant, the NO concentration does not change significantly with the increase of tertiary air temperature.

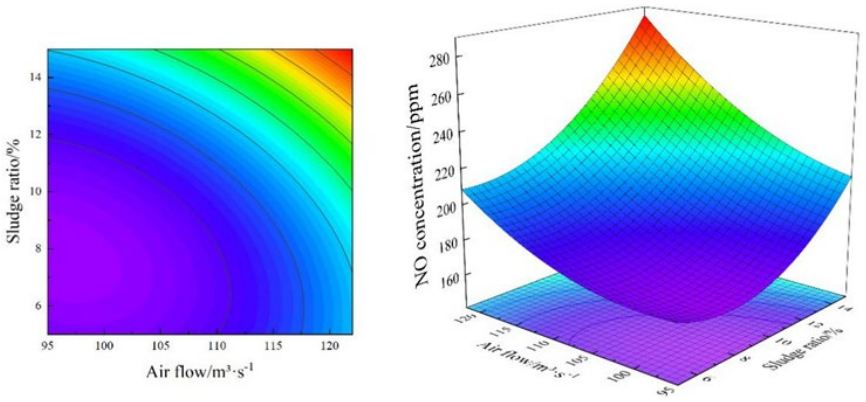

Fig. 6. Response surface of combined effects of sludge input ratio and airflow on NO concentration

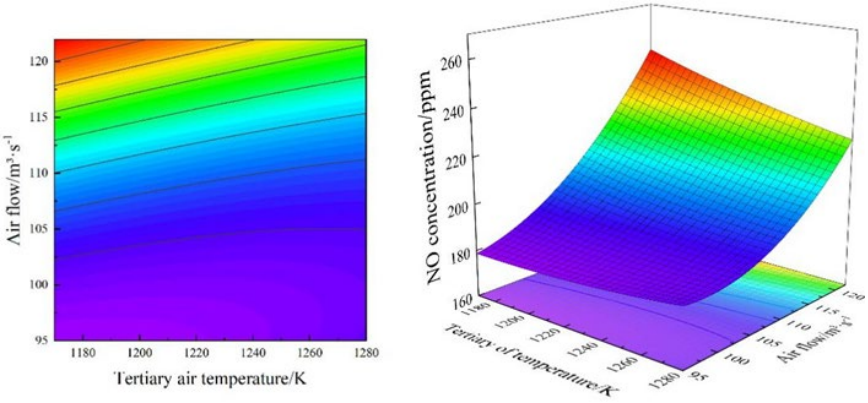

Fig. 7. Response surface of combined effects of tertiary air temperature and airflow on NO concentration

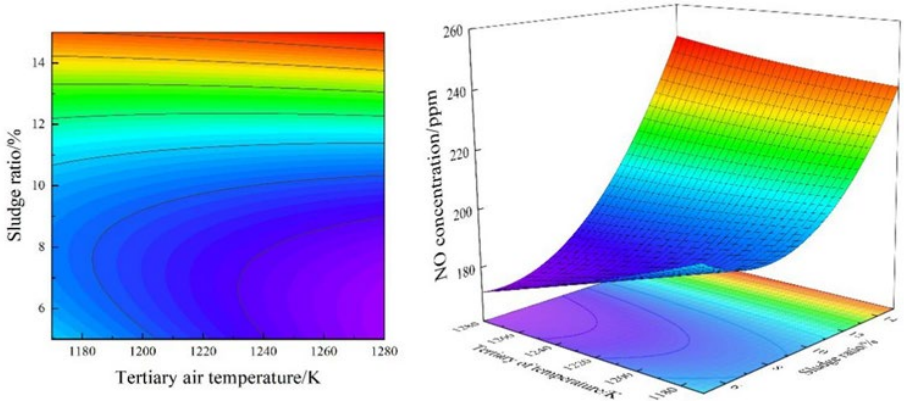

Fig. 8. Response surface of combined effects of tertiary air temperature and sludge input ratio on NO concentration

The NO concentration exhibits an increasing trend with increased airflow at constant tertiary air temperatures. However, the NO concentration is not significantly affected by the combination of tertiary air temperatures and air movement.

Figure 8 shows the dependences of the tertiary air temperatures and sludge input ratio on the NO concentration. As can be seen from Fig. 8b, the NO concentration does not change much as the tertiary air temperatures increase at a constant sludge input ratio. When the tertiary air temperatures are fixed, the NO concentration gradually increases with the increase of the sludge ratio. The sludge input ratio and tertiary air temperatures have some effect on the NO concentration.

The interaction between airflow (X_2) and sludge input ratio (X_1) is more significant than that between sludge input ratio (X_1) and tertiary air temperature (X_3), and is also more dramatic than that between airflow (X_2) and tertiary air temperature (X_3) Figs. 6–8). As a consequence, sludge addition and airflow have a large effect on NO production.

4.3. RESPONSE SURFACE MODEL OPTIMIZATION

The model is improved by eliminating the two irrelevant components X_2X_3 and X_3X_3 to make the response surface more representative.

$$y = 185.45 + 28.79X + 27.48X_2 - 4.74X_3 + 9.52X_1X_2 + 9.74X_1X_3 + 21.51X_1^2 + 12.33X_2^2$$

The optimized model is when $P < 0.0001$, R^2 is 97.92%, and R^2(adj) is 95.84% with statistical significance. The best conditions for NO concentration are 5% sludge ratio, 109 m³/s airflow, and 1280 K tertiary air temperature. Under those conditions, NO concentration is 166.9 mg/m³ and the simulated value is quite close – 166.3 mg/m³.

5. CONCLUSION

- The sludge ratio influences the composition of the fuel. The NO concentration gradually increases with the increase of the furnace temperature, and the maximum NO concentration is 297 mg/m³ at the sludge input ratio of 20%.
- When the airflow increases, the oxygen content at the furnace outlet gradually increases, and NO concentration increases as well.
- Due to the increase in the tertiary air temperature, the fuel is prompted to burn fully, releasing more HCN and NH_3, reducing NO to a certain extent, and decreasing NO concentration.
- The experimental conditions have been optimized by the investigations of the effect of three factors on NO concentration. The best condition is the sludge proportion of 5%, airflow of 109 m³/s, and tertiary air temperature of 1280 K. The NO concentration is then 166.9 mg/m³, and the simulated value 166.3 mg/m³. The validation results show

that the model can predict the NO concentration under various sludge ratios, airflow, and tertiary air temperatures.

ACKNOWLEDGEMENTS

This work was supported by the National Natural Science Foundation of China (U20A20130).

REFERENCES

[1] TANG Z., FANG P., XIAO X., HUANG J., CHEN X., ZHONG P., TANG Z., CEN C., *Data on species and concentration of the main gaseous products during sludge combustion to support the feasibility of using sludge as a flue gas denitration agent for the cement industry*, Data Brief, 2019, 25, 103998. DOI: 10.1016/j.dib.2019.103998.

[2] LIANG Y., XU D., FENG P., HAO B., GUO Y., WANG S., *Municipal sewage sludge incineration and its air pollution control*, J. Clean. Prod., 2021, 295 (3), 126456. DOI: 10.1016/j.jclepro.2021.126456.

[3] LIAO Y.F., MA X.Q., *Thermogravimetric analysis of the co-combustion of coal and paper mill sludge*, Appl. En., 2010, 87 (11), 3526–3532. DOI: 10.1016/j.apenergy.2010.05.008.

[4] TREZZA M.A., SCIAN A.N., *Waste fuels. Their effect on Portland cement clinker*, Cem. Concr. Res., 2005, 35 (3), 438–444. DOI: 10.1016/j.cemconres.2004.05.045.

[5] CHEN H., YAN S.H., YE Z.L., MENG H.J., ZHU Y.G., *Utilization of urban sewage sludge: Chinese perspectives*, Environ. Sci. Poll. Res., 2012, 19 (5), 1454–1463. DOI: 10.1007/s11356-012-0760-0.

[6] YANG Y., ZHANG Y., LI S., LIU R., DUAN E., *Numerical simulation of low nitrogen oxides emissions through cement precalciner structure and parameter optimization*, Chemosphere, 2020, 258, 127420. DOI: 10.1016/j.chemosphere.2020.127420.

[7] HOUSHFAR E., LØVÅS T., SKREIBERG Ø., *Experimental investigation on NO_x reduction by primary measures in biomass combustion. Straw, peat, sewage sludge, forest residues and wood pellets*, Energ., 2012, 5 (2), 270–290. DOI: 10.3390/en5020270.

[8] SHIMIZU T., TOYONO M., OHSAWA H., *Emissions of NO_x and N_2O during co-combustion of dried sewage sludge with coal in a bubbling fluidized bed combustor*, Fuel, 2007, 86 (7–8), 957–964. DOI: 10.1016/j.fuel.2006.10.001.

[9] XIAO X., LUO J., HUANG H., XU Z., WU H., HUANG J., FANG P., *Study on the influencing factors of removal of NO_x from cement kiln flue gas by sewage sludge as a denitration agent*, Environ. Sci. Poll. Res. Int., 2020, 27 (33), 41342–41349. DOI: 10.1007/s11356-020-10126-2.

[10] LV D., ZHU T., LIU R., LV Q., SUN Y., WANG H., LIU Y., ZHANG F., *Effects of co-processing sewage sludge in cement kiln on NO_x, NH_3 and PAHs emissions*, Chemosphere, 2016, 159, 95–601. DOI: 10.1016/j.chemosphere.2016.06.062.

[11] FANG P., TANG Z., XIAO X., HUANG J., CHEN X., ZHONG P., TANG Z., CEN C., *Using sewage sludge as a flue gas denitration agent for the cement industry: Factor assessment and feasibility*, J. Clean. Prod., 2019, 224, 292–303. DOI: 10.1016/j.jclepro.2019.03.175.

[12] XIAO X., FANG P., HUANG J.-H., TANG Z.-J., CHEN X.-B., WU H.-W., CEN C.-P., TANG Z.-X., *Mechanistic study on NO reduction by sludge reburning in a pilot scale cement precalciner with different CO_2 concentrations*, RSC Adv., 2019, 9 (40), 22863–22874. DOI: 10.1039/D0RA90006K.

[13] WANG W., LIAO Y., LIU J., HUANG Z., TIAN M., *Numerical simulation and optimization of staged combustion and no_x release characteristics in precalciner*, J. Therm. Sci., 2019, 28 (5), 1024–1034. DOI: 10.1007/s11630-019-1164-y.

[14] SU S., XIANG J., SUN L., ZHANG Z., SUN X., ZHENG C., *Numerical simulation of nitric oxide destruction by gaseous fuel reburning in a single-burner furnace*, Proc. Combust. Inst., 2007, 31 (2), 2795–2803. DOI: 10.1016/J.PROCI.2006.07.260.

[15] YIN C., YAN J., *Oxy-fuel combustion of pulverized fuels. Combustion fundamentals and modeling*, Appl. En., 2016, 162, 742–762. DOI: 10.1016/j.apenergy.2015.10.149.

[16] FIDAROS D.K., BAXEVANOU C.A., DRITSELIS C.D., VLACHOS N.S., *Numerical modelling of flow and transport processes in a calciner for cement production*, Powder Technol., 2007, 171 (2), 81–95. DOI: 10.1016/j.powtec.2006.09.011.

[17] BAUM M.M., STREET P.J., *Predicting the combustion behaviour of coal particle*s, Comb. Sci. Technol., 1971, 3 (5), 231–243. DOI: 10.1080/00102207108952290.

[18] FIELD M.A., R*ate of combustion of size-graded fractions of char from a low-rank coal between 1200 K and 2000 K*, Comb. Flame, 1969, 13 (3), 237–252. DOI: 10.1016/0010-2180 (69)90002-9.

[19] CHOI C.R., KIM C.N., *Numerical investigation on the flow, combustion and NO_x emission characteristics in a 500 MWe tangentially fired pulverized-coal boiler*, Fuel, 2009, 88 (9), 1720–1731. DOI: 10.1016 /j.fuel.2009.04.001.

[20] GHENAI C., INAYAT A., SHANABLEH A., AL-SARAIRAH E., JANAJREH I., *Combustion and emissions analysis of Spent Pot lining (SPL) as alternative fuel in cement industry*, Sci. Total. Environ., 2019, 684, 519–526. DOI: 10.1016/j.scitotenv.2019.05.157.

[21] NAKHAEI M., WU H., GRÉVAIN D., JENSEN L.S., GLARBORG P., DAM-OHANSEN K., *CPFD simulation of petcoke and SRF co-firing in a full-scale cement calciner*, Fuel Process. Technol., 2019, 196. DOI: 10.1016/j.fuproc.2019.106153.

[22] HU Z., MA X., CHEN Y., LIAO Y., WU J., YU Z., LI S., YIN L., XU Q., *Co-combustion of coal with printing and dyeing sludge: Numerical simulation of the process and related NO_x emissions*, Fuel, 2015, 139, 606–613. DOI: 10.1016/j.fuel.2014.09.047.

[23] ZHANG J., TIAN Y., ZHU J., ZUO W., YIN L., *Characterization of nitrogen transformation during microwave-induced pyrolysis of sewage sludge*, J. Anal. Appl. Pyrol., 2014, 105, 335–341. DOI: 10.1016 j.jaap.2013.11.021.

[24] LI X., ZENG L., LIU H., DU H., YANG X., HAN H., LIU W., ZHANG S., SONG M., CHEN Z., LI Z., *Numerical simulation study on the influences of the secondary-tertiary air proportion on the airflow mixing effects and pulverized coal combustion characteristics in a 300-MW down-fired boiler*, Proc. Saf. Environ. Prot., 2019, 130, 326–343. DOI: 10.1016/j.psep.2019.08.022.

[25] ESTRADA-VAZQUEZ C., SALINAS-PACHECO A., PERALTA-REYES E., POGGI-VARALDO H.M., REGALADO--MENDEZ A., *Parametric optimization of domestic wastewater treatment in an activated sludge sequencing batch reactor using response surface methodology*, J. Environ. Sci. Health, A, Tox. Hazard. Subst. Environ. Eng., 2019, 54 (12), 1197–1205. DOI: 10.1080/10934529.2019.1631087.